Eur. Phys. J. D **3**, 67–71 (1998)

THE EUROPEAN
PHYSICAL JOURNAL D

© EDP Sciences
Springer-Verlag 1998

Elastic scattering of low-energy electrons by $N_2O^\star$

S.M.S. da Costa and M.H.F. Bettega[a]

Departamento de Física, Universidade Federal do Paraná, UFPR, Caixa Postal 19081, 81531-990 Curitiba, Paraná, Brazil

Received: 13 November 1997 / Revised: 13 March 1998 / Accepted: 9 April 1998

Abstract. We report elastic integral, momentum transfer and differential cross sections for electron scattering by N_2O for energies up to 50 eV. These results were obtained at the static-exchange approximation with the Schwinger Multichannel Method with Pseudopotentials [M.H.F. Bettega, L.G. Ferreira and M.A.P. Lima, Phys. Rev. A **47**, 1111 (1993)]. In general our results show good agreement with experimental data and with other theoretical results but some discrepancies are found. We have also found a $^2\Pi$ shape resonance around 4 eV in agreement with previous calculations using the *R*-matrix Method of Sarpal *et al.* [J. Phys. B **29**, 857 (1996)]. On the other hand, the existence of a $^2\Sigma$ resonance at about 13 eV, clearly seen by the Schwinger Variational Iterative Method [Michelin *et al.*, J. Phys. B **29**, 2115 (1996)], can not be confirmed by our calculations. At this energy, our $^2\Sigma$ cross sections show a broad bump with no clear resonant behavior given by the eigenphase sum.

PACS. 34.80.Bm Elastic scattering of electrons by atoms and molecules – 34.80.Gs Molecular excitation and ionization by electron impact

1 Introduction

The modeling of the basic processes that occur in a discharge environment, that are used to generate cold plasmas, involves the knowledge of the elastic and inelastic cross sections resulting from the collisions of the low-energy electrons and the molecules present in this environment. To deal with such a problem, there are several methods in current use that are able to give reliable cross sections [1,2]. However, due to computer limitations, the applications of these methods have been restricted to linear and small polyatomics targets.

The simplification of the scattering calculations has been proposed recently with the implementation of soft norm-conserving pseudopotentials [3] (PP) into the Schwinger multichannel method [4,5]. The role played by the PP is to replace the core electrons of each atom in a molecule, and only the valence electrons are considered in the calculations. Besides, the norm-conserving PP produce valence wave functions that are smooth and nodeless, and as a consequence they can be fitted with basis sets containing a small number of functions (in our case Cartesian Gaussian functions). Several applications of this method have been done in elastic and inelastic calculations [6]. Norm-conserving PP have also been implemented in the Kohn method [7].

In the last years, several studies concerning scattering of electrons against N_2O have been done due to its application in lasers, cold plasmas and the upper atmosphere. Measurements of total cross sections [8,9], elastic integral and differential cross sections [10–12] have been performed as well as calculations of integral and differential cross sections [13–15]. Sarpal *et al.* [13] applied the polyatomic *R*-matrix method to study elastic scattering of electrons by N_2O at the static-exchange and at the static-exchange plus polarization levels of approximation, in order to study the shape resonance that they found to be due to the $^2\Pi$ state of the negative ion. They also studied the influence of the target correlation in the description of this resonance. A $^2\Sigma$ shape resonance around 10 eV was found when they included polarization effects in their calculation. Michelin *et al.* [14] applied the Schwinger variational iterative method to study elastic scattering of electrons by N_2O at the static-exchange approximation and the distorted-wave method to study electronic excitation to the lowest $^{1,3}\Pi$ states of N_2O by electron impact at the 2-state level of approximation. In their static-exchange calculations they found a shape resonance around 13 eV at the $^2\Sigma$ channel from $l = 1$. Morgan *et al.* [15] applied a polyatomic code, also based on the *R*-Matrix method, to study the $^2\Pi$ shape resonance. Their static-exchange results agree with those of Sarpal *et al.*, but they have not found any $^2\Sigma$ resonance below 10 eV, even when they included polarization effects. In this paper we report integral, momentum transfer and differential cross sections for elastic scattering of low-energy electrons by N_2O for energies up to 50 eV. We have used the Schwinger multichannel method with pseudopotentials (SMCPP) at the static-exchange (SE) approximation. Since N_2O has a small permanent dipole

---

* Dedicated to Prof. Luiz Guimarães Ferreira on the occasion of his 60th birthday

[a] e-mail: `bettega@fisica.ufpr.br`

moment, we did not use the standard Born closure to complete the scattering amplitude in order to describe the higher partial waves, as Michelin *et al.* [14] did. The SMC (SMCPP) method uses only L^2 functions to describe the scattering wave function and therefore the long range potential due to the dipole interaction in truncated. As a result the differential cross sections are meaningful above certain scattering angles (the DCS diverges in a forward direction) [16,17].

This paper is outlined as follows. The theoretical formulation of SMC (SMCPP) method is presented in Section 2. Section 3 presents the computational procedures. The results and discussion are presented in Section 4. Section 5 ends with a brief summary.

2 Theoretical formulation

The SMC [4,18] and SMCPP [5] methods have been discussed in earlier works, and we will review here only some key steps of these methods. The SMC method is a multichannel extension of the Schwinger variational principle. Actually it is a variational approximation for the scattering amplitude, where the scattering wave function is expanded in a basis of $(N+1)$-particle Slater determinants

$$|\Psi_{\mathbf{k}}\rangle = \sum_m a_m^{\pm}(\mathbf{k})|\chi_m\rangle \tag{1}$$

and the coefficients $a_m^{\pm}(\mathbf{k})$ of this expansion are then variationally determined. The resulting expression for the scattering amplitude in the body frame is

$$[f_{\mathbf{k}_i,\mathbf{k}_f}] = -\frac{1}{2\pi}\sum_{m,n}\langle S_{\mathbf{k}_f}|V|\chi_m\rangle(d^{-1})_{mn}\langle\chi_n|V|S_{\mathbf{k}_i}\rangle \tag{2}$$

where

$$d_{mn} = \langle\chi_m|A^{(+)}|\chi_n\rangle \tag{3}$$

and

$$A^{(+)} = \frac{\hat{H}}{N+1} - \frac{(\hat{H}P + P\hat{H})}{2} + \frac{(VP+PV)}{2} - VG_P^{(+)}V. \tag{4}$$

In the above equations $S_{\mathbf{k}_i}$, solution of the unperturbed Hamiltonian H_0, is the product of a target state and a plane wave, V is the interaction potential between the incident electron and the target, $|\chi_m\rangle$ is an $(N+1)$-electron Slater determinant used in the expansion of the trial scattering wave function, $\hat{H} = E - H$ is the total energy of the collision minus the full Hamiltonian of the system, with $H = H_0 + V$, P is a projection operator onto the open-channel space defined by target eigenfunctions $|\Phi_l\rangle$

$$P = \sum_l^{open} |\Phi_l\rangle\langle\Phi_l| \tag{5}$$

and $G_P^{(+)}$ is the free-particle Green's function projected on the P-space.

For elastic scattering at the static-exchange approximation, the P operator is composed only by the ground state of the target $|\Phi_1\rangle$

$$P = |\Phi_1\rangle\langle\Phi_1| \tag{6}$$

and the configuration space $|\chi_m\rangle$ is

$$\{|\chi_m\rangle\} = \mathcal{A}|\Phi_1\rangle|\varphi_i\rangle \tag{7}$$

where $|\varphi_i\rangle$ is a 1-particle function represented by one molecular orbital.

With the choice of Cartesian Gaussian functions to represent the molecular and scattering orbitals, all the matrix elements arising in equation (2) can be computed analytically, except those from $\langle\chi_m|VG_P^{(+)}V|\chi_n\rangle$ (VGV), that are evaluated by numerical quadrature [18].

The numerical calculation of the matrix elements from VGV represent the more expensive step in the SMC code and demand almost the entire computational time of the scattering calculation. These matrix elements are reduced to a sum of primitive two-electron integrals involving a plane wave and three Cartesian Gaussians

$$\langle\alpha\beta|V|\gamma\mathbf{k}\rangle = \int\int d\mathbf{r}_1 d\mathbf{r}_2 \alpha(\mathbf{r}_1)\beta(\mathbf{r}_1)\frac{1}{r_{12}}\gamma(\mathbf{r}_2)e^{i\mathbf{k}\cdot\mathbf{r}_2} \tag{8}$$

and must be evaluated for all possible combinations of α, β and γ and for several directions and moduli of $\mathbf{k}$. We must also evaluate the one-electron integrals of the type

$$\langle\alpha|V^{PP}|\mathbf{k}\rangle = \int d\mathbf{r}\alpha(\mathbf{r})V^{PP}e^{i\mathbf{k}\cdot\mathbf{r}}. \tag{9}$$

These one-electron integrals are more complex than those involving the nuclei, but they can be calculated analytically and their number is also reduced due to the smaller basis set. In the above equation, V^{PP} is the nonlocal pseudopotential operator given by:

$$\hat{V}^{PP}(r) = \hat{V}_{core}(r) + \hat{V}_{ion}(r), \tag{10}$$

with

$$\hat{V}_{core}(r) = -\frac{Z_v}{r}\left[\sum_{i=1}^{2} c_i^{core}\mathrm{erf}\left[(\alpha_i^{core})^{1/2}r\right]\right], \tag{11}$$

and

$$\hat{V}_{ion}(r) = \sum_{n=0}^{1}\sum_{j=1}^{3}\sum_{l=0}^{2} A_{njl}r^{2n}e^{-\alpha_{jl}r^2}\sum_{m=-l}^{+l}|lm\rangle\langle lm|, \tag{12}$$

where Z_v is the valence charge of the atom and in this application it is equal to 5 for N, and 6 for O. The coefficients c_i^{core}, A_{njl}, and the decay constants α_i^{core} and α_{jl} are tabulated in reference [3].

Even for small molecules, a large number of the two-electron integrals must be evaluated. This limits the size of molecules in scattering calculations. In the SMCPP method we need shorter basis set to describe the target and scattering and consequently the number of two electron integrals is smaller than in the all-electron case. The reduction in the number of these integrals allows the study of larger molecules than those reachable by all-electron techniques.

Table 1. Cartesian Gaussian functions (defined by $\phi_{lmn} = N_{lmn}(x-a_x)^l(y-a_y)^m(z-a_z)^n \exp(-\alpha|\mathbf{r}-\mathbf{a}|^2)$) for nitrogen and oxigen.

	N	O	
Type	Exponent	Exponent	Coefficient
s	17.567340	16.058780	1.0
s	3.423615	5.920242	1.0
s	0.884301	1.034907	1.0
s	0.259045	0.316843	1.0
s	0.055708	0.065203	1.0
p	7.050692	10.141270	1.0
p	1.910543	2.783023	1.0
p	0.579261	0.841010	1.0
p	0.165395	0.232940	1.0
p	0.037192	0.052211	1.0
d	0.403039	0.756793	1.0
d	0.091192	0.180759	1.0

3 Computational procedures

The ground state of the N_2O molecule is described by the valence electronic configuration $4\sigma^2\ 5\sigma^2\ 6\sigma^2\ 1\pi^4\ 7\sigma^2\ 2\pi^4$ ($X^1\Sigma^+$). The basis functions we used in the description of the valence part of the target state $|\Phi_1\rangle$ and to describe the scattering orbitals $|\varphi_i\rangle$ are shown in Table 1. These functions were generated by a variational procedure [19], being suitable for these pseudopotential calculations. Our calculated dipole moment is 0.63 Debye and the results of references [13,14] are 0.87 and 0.68 Debye respectively. The experimental dipole moment is 0.16 Debye. All calculations were performed in a fixed-nuclei static-exchange approximation at the experimental equilibrium geometry.

4 Results and discussion

In Figure 1 we present our calculated integral cross section. We compare our results with the theoretical results of Sarpal *et al.*, obtained with the polyatomic R-matrix method at the static-exchange approximation, with the theoretical results of Michelin *et al.* [14], obtained with the Schwinger variational iterative method (SVM), with total cross section measurements from reference [8] and with elastic cross section data from references [10,11], obtained by the integration of the (extrapolated) differential cross sections. We have not included the SE results of Morgan *et al.* [15], obtained with a polyatomic code also based on the R-Matrix method, because these results are very close to those of Sarpal *et al.* Our results agree, at low energies, with the results of Sarpal *et al.*, that includes only the contribution of Π and Σ symmetries, and for $E \geq 10$ eV with the experimental data. The theoretical results of Michelin *et al.* lie above all the other results, except at high energies, where they cross the results of reference [8]. They found a resonant behavior around 13 eV. For $E < 10$ eV, the discrepancies between theory and experiment are, in principle, due to the polarization effects that are not take into account in these calculations. The integral cross section of Sarpal *et al.* show some structures above 10 eV. These structures do not appear in our results nor in other results shown in Figure 1. In particular, our results follow the shape of total cross section measurements of reference [8], and agree very well with them for $E \geq 10$ eV, indicating that the elastic cross section gives the major part of the total cross section. The the sum of the Π and the Σ symmetries gives the major part of the elastic cross section, as the results of Sarpal *et al.* [13] shown.

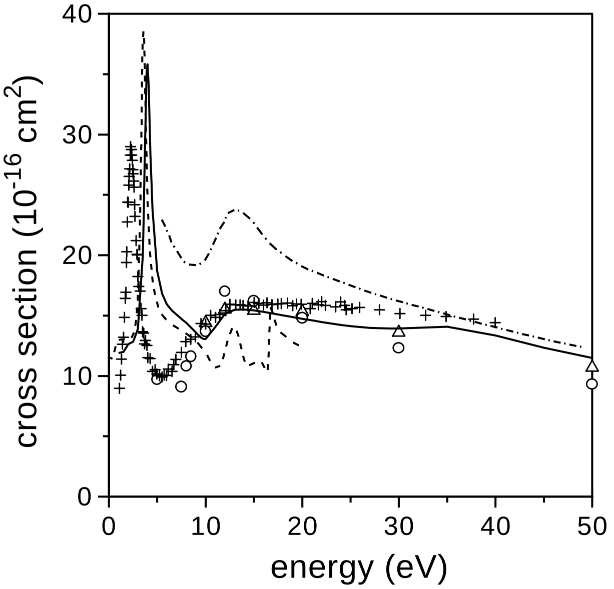

Fig. 1. Integral cross section for N_2O. Solid line, our results; dotted-dashed, theoretical results from reference [14]; dashed line, results from reference [13]; triangles, experimental results from reference [10]; circles, experimental results from reference [11], crosses, experimental results from reference [8].

In Figures 2 and 3 we show the symmetry decomposition of the integral cross section of Figure 1 for Π and Σ symmetries, where the inset in each figure shows the respective eigenphase sum, and compare with the results of Sarpal *et al.* We also found a $^2\Pi$ shape resonance around 4 eV, as shows our calculated eigenphase sum. Although the position of the resonances are slightly shifted between each other and apart from the structures that appear in the polyatomic R-matrix results, there is good agreement between both calculations. Our $^2\Sigma$ cross sections show a broad bump around 10 eV with no clear resonant behavior given by the eigenphase sum.

Figure 4 shows our momentum transfer cross section and the experimental data of references [11,10]. Our results describes correctly the shape of the experimantal data, but the agreement is only qualitative. The momentum transfer cross sections from references [11,10] were obtained by the integration of the extrapolated DCS. In Figures 5, 6 and 7 we show our differential cross sections (DCS) at 5, 7.5, 8, 10, 12, 15, 20, 30 and 50 eV. We found good agreement with experimental data, except at low energies ($E < 10$ eV) and low scattering angles ($\theta \lesssim 30°$), where our results deviate from the experimental data. In our calculations we do not include polarization effects nor complete the scattering amplitude with the Born closure

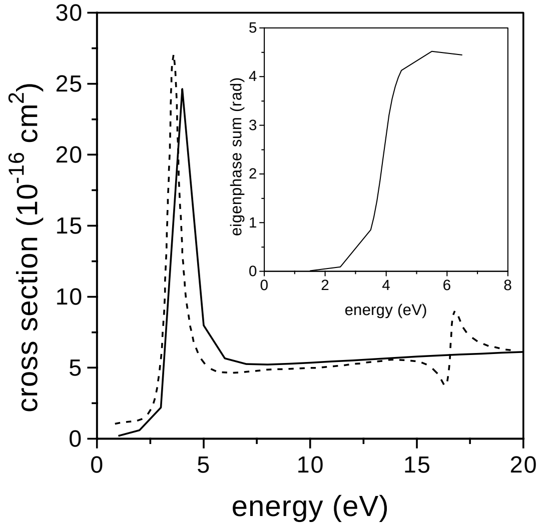

Fig. 2. Partial decomposition of the integral cross section for the Π symmetry. Solid line, our results; dashed line, results from reference [13]. The inset shows the eigenphase sum.

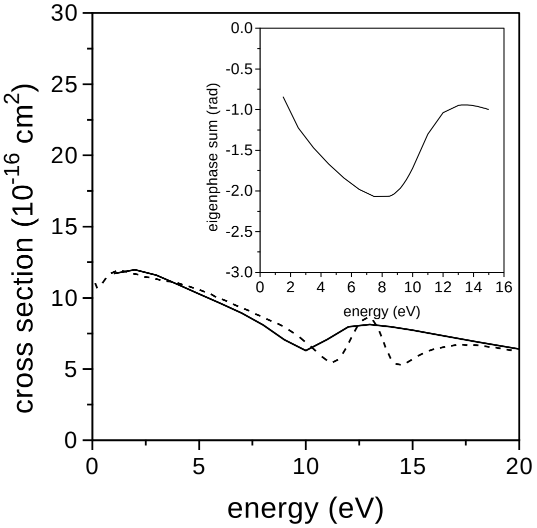

Fig. 3. As in Figure 2 for the Σ symmetry.

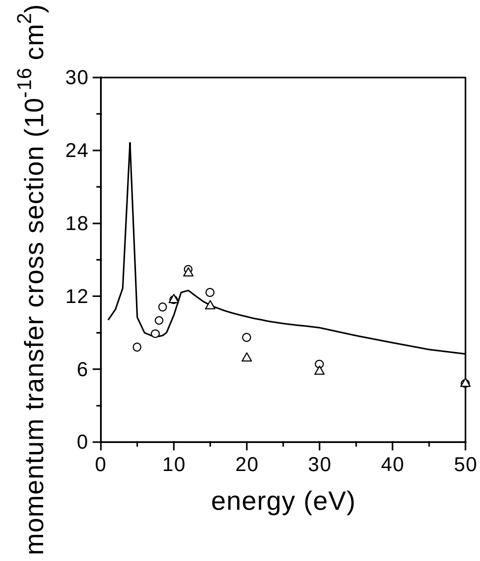

Fig. 4. Momentum transfer cross section. Solid line, our results; triangles, experimental results from reference [10]; circles, experimental results from reference [11].

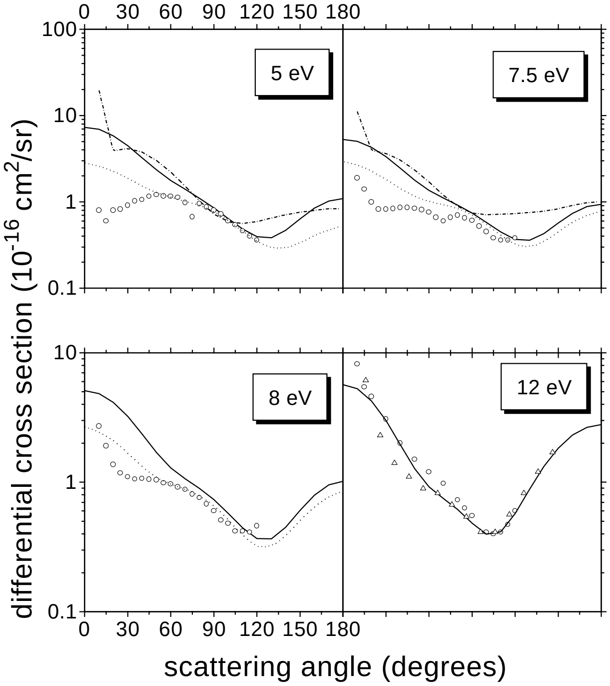

Fig. 5. Differential cross sections for N_2O at 5, 7.5, 8 and 12 eV. Solid line, our results; dotted-dashed line, theoretical results from reference [14]; dotted line, theoretical results from reference [15]; triangles, experimental results from reference [10]; circles, experimental results from reference [11].

to describe the higher partial waves. The lack of polarization effects explains the differences, in the DCS, between our results and the experimental data below 10 eV. The lack of the dipole potential (included *via* Born closure) explains the differences at low scattering angles. Michelin *et al.* have combine their SVM amplitude with Born closure and therefore they should be able to reproduce the DCS at low scattering angles, for energies where polarization is not important. We found good agreement between our DCS and the calculated DCS of Michelin *et al.* only for $E \geq 30$ eV. In our opinion, the results of Michelin *et al.* are not fully converged. At 30 eV both theoretical results agree very well with each other but diverge from experiment at high scattering angles. In general, the SE approximation works very well at this energy and this discrepancies may not be attributed, at least in principle, to this approximation. We have also observed this kind of discrepancies in other molecules, as in H_2S, for example. Although our calculations do not include polarization effects, our static-exchange DCS in general agree with the DCS of Morgan *et al.*, that include polarization effects.

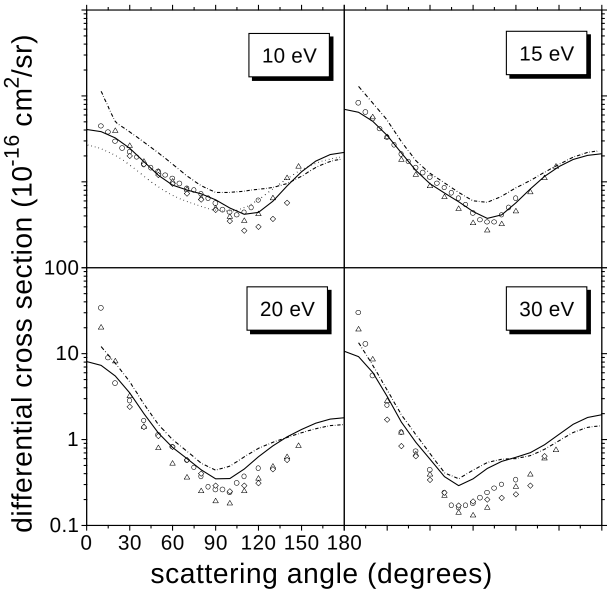

Fig. 6. Differential cross sections for N_2O at 10, 15, 20 and 30 eV. Solid line, our results; dotted-dashed line, theoretical results from reference [14]; dotted line, theoretical results from reference [15]; triangles, experimental results from reference [10]; circles, experimental results from reference [11]; diamonds, experimental results from reference [12].

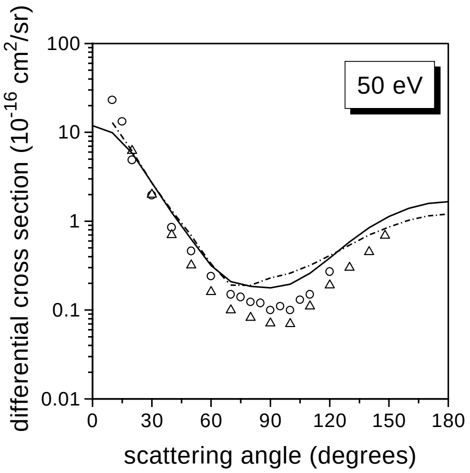

Fig. 7. Differential cross sections for N_2O at 50 eV. Solid line, our results; dotted-dashed line, theoretical results from reference [14]; triangles, experimental results from reference [10]; circles, experimental results from reference [11].

5 Summary

In this paper we reported calculated integral, momentum transfer and differential cross sections for scattering of low-energy electrons by N_2O at the static-exchange level of approximation. We have used the Schwinger multichannel method with pseudopotentials. We found reasonably good agreement with with experimental data and with other theoretical results. We found that the elastic cross section is responsible for the major part of the total cross section, and that the shape resonance is due to a $^2\Pi$ state of the negative ion, which agree with the previous calculations of Sarpal *et al.*

S.M.S.C acknowledges Brazilian agency Conselho Nacional de Desenvonvimento Científico e Tecnológico (CNPq) for the support from the program PIBIC/CNPq. M.H.F.B. acknowledges partial support from FUNPAR and CNPq. Our calculations were performed at CENAPAD-SP, at CENAPAD-NE and at CCE-UFPR. The authors would like to thank Dr. M.A.P. Lima and Dr M-T Lee for insightfull discussions concerning this work.

References

1. See, for example, *Modern Electronic Structure Theory*, edited by D.R. Yarkony (World Scientific, 1995) chapters 9 and 22; A. Garscadden, Z. Phys. D **24**, 99 (1992).
2. See, for example, *Computational Methods for Electron-Molecule Collisions*, edited by W.M. Huo, F.A. Gianturco (Plenum, 1995).
3. G. Bachelet, D.R. Hamann, M. Schlüter, Phys. Rev. B **46**, 4199 (1982).
4. K. Takatsuka, V. McKoy, Phys. Rev. A **24**, 2473 (1981); *ibid.* **30**, 1734 (1984).
5. M.H.F. Bettega, L.G. Ferreira, M.A.P. Lima, Phys. Rev. A **47**, 1111 (1993).
6. A.P.P. Natalense, M.H.F. Bettega, L.G. Ferreira, M.A.P. Lima, Phys. Rev. A **52**, R1 (1995); M.H.F. Bettega, A.P.P. Natalense, M.A.P. Lima, L.G. Ferreira, J. Chem. Phys. **103**, 10566 (1995); A.P.P. Natalense, C.S. Sartori, L.G. Ferreira, M.A.P. Lima, Phys. Rev. A **54**, 5435 (1996); M.T. do N. Varella, M.H.F. Bettega, M.A.P. Lima, Z. Phys. D **39**, 59 (1997).
7. T.N. Rescigno, C.W. McCurdy, J. Chem. Phys. **104**, 120 (1996).
8. Cz Szmytkowski, G. Karwasz, K. Maciag, Chem. Phys. Lett. **107**, 481 (1984)
9. Cz Szmytkowski, K. Maciag, G. Karwasz, D. Filipović, J. Phys. B **27**, 525 (1989).
10. B. Marinković, Cz Szmytkowski, V. Pejcev, D. Filipović, L. Vusković, J. Phys. B **19**, 2365 (1986).
11. W.M. Johnstone, W.R. Newell, J. Phys. B **26**, 129 (1993).
12. M. Kubo, D. Matsunaga, T. Suzuki, H. Tanaka, *Proc. 12th Int. Conf. on Physics of Electronic and Atomic Collisions*, edited by S. Datz, North Holland, abstracts p. 360.
13. B.K. Sarpal, K. Pfingst, B.M. Nestmann, and S.D. Peyerimhoff, J. Phys. B **29**, 857 (1996).
14. S.E. Michelin, T. Kroin, M.T. Lee, J. Phys. B **29**, 2115 (1996).
15. L.A. Morgan, C.J. Gillan, J. Tennyson, X. Chen, J. Phys. B **30**, 4087 (1997).
16. C. Winstead, Q. Sun, V. McKoy, J. Chem. Phys. **96**, 4246 (1992).
17. M.H.F. Bettega, M.A.P. Lima, L.G. Ferreira, J. Chem. Phys. **105**, 1029 (1996).
18. M.A.P. Lima, L.M. Brescansin, A.J.R. da Silva, C. Winstead, V. McKoy, Phys. Rev. A **41**, 327 (1990).
19. M.H.F. Bettega, A.P.P. Natalense, M.A.P. Lima, L.G. Ferreira, Int. J. Quantum Chem. **60**, 821 (1996).